POINT PROCESS MODELLING OF ROOT DISTRIBUTION IN PURE STANDS OF *FAGUS SYLVATICA* AND *PICEA ABIES*

F. FLEISCHER [1,2], S. ECKEL [2], I. SCHMID [3], V. SCHMIDT [2], and M. KAZDA [3]

[1]Department of Applied Information Processing
University of Ulm, D-89069 Ulm, Germany

[2]Department of Stochastics
University of Ulm, D-89069 Ulm, Germany

[3]Department of Systematic Botany and Ecology
University of Ulm, D-89069 Ulm, Germany

Corresponding author:
Frank Fleischer
Department of Applied Information Processing & Department of Stochastics
University of Ulm, D-89069 Ulm, Germany
Phone : +49 731 50 23617
Fax : +49 731 50 23649
E-mail: Frank.Fleischer@uni-ulm.de

ABSTRACT

Previous study by Schmid & Kazda (2001) evaluated vertical distribution and radial growth of coarse roots above 2 *mm* diameter in pure and mixed stands of Norway spruce (*Picea abies* L.) and European beech (*Fagus sylvatica* (L.) Karst.) (Can. J. For. Res. **31**: 539-548). The vertical distribution of roots of Norway spruce was fitted by an exponential function, while the root distribution of European beech was approximated by a gamma distribution. Now, in the present paper, planar point-process models have been applied to investigate the spatial (two-dimensional) distribution of root data between 2 *mm* and 5 *mm* diameter. After a homogenization with respect to the vertical axis, the pair correlation function and the *L*-function have been estimated in order to fit Matérn-cluster point process models to the given root data. The models were finally vertically retransformed to provide information about the inhomogeneous spatial patterns of the small roots also regarding the original shape and size of the root clusters. All models on the vertically transformed data confirmed that the root distribution patterns are not completely random, indicating root clustering for both species with different degree of exploitation intensity (clustering) between the two species. According to the Matérn-cluster models, *Picea abies* had stronger clustering in smaller cluster regions, while roots of *Fagus sylvatica* formed weaker clusters in larger cluster regions. Furthermore, beech root clusters seem to avoid an overlap. Together with previous studies on the root system of both species, this indicates more intensive below-ground intraspecific competition for spruce than for beech. On the other hand the clustering characteristics described indicate a more sophisticated rooting system of European beech compared to Norway spruce. Regarding the spatial distribution of the inhomogeneous raw data, there is a combination of the clustering properties analysed in the present paper and the vertical distribution already known.

Keywords: Matérn-cluster process, model fitting, planar point pattern, Poisson process, root clustering;

1. INTRODUCTION

Vertical root distribution can be described as a one-dimensional depth function (Parker & van Lear 1996) with the greatest root density in the top soil layers for most forests (Jackson & Caldwell 1996). Besides the vertical distribution, early studies assumed that the rooting zone is completely and almost homogeneously exploited by roots (Krauss et al. 1939). Recent studies in natural ecosystems found, however, that fine roots concentrate in distinct soil patches (Caldwell et al. 1996; Hölscher et al. 2002; Pellerin & Pages 1996; Ryel et al. 1996). Several experiments with small plants (Facelli & Facelli 2002; Linkohr et al. 2002; Wijesinghe & Hutschings 1997) have shown that plants respond by proliferation of fine roots into zones of nutrient enrichment and water availability, thus producing a patched root distribution. As the resources in natural soils are most abundant in the topsoil, fine roots abundance still follows the vertical distribution function but on the horizontal scale heterogeneity of root abundance can be expected in line with unevenly distributed soil resources.

Bouillet et al. (2002) found large spatial heterogeneity and clusters of fine roots in a clonal Eucalyptus plantation independently from the distance to the planting row. The study also confirmed that more knowledge is required about the root distribution of intermediate root classes between 2 mm and 20 mm diameter, because recent studies showed water and nutrient uptake also for these roots (Lindenmair et al. 2001).

Trench soil profiles can be used for the assessment of two-dimensional root distribution, where roots on the wall can be seen as points of different diameter. Previous evaluation methods counted the roots within a grid cell (Böhm 1976; Bouillet et al. 2002) or just evaluated the presence or absence of roots (Tardieu 1988). A new assessment method (Schmid & Kazda 2001) provided (x, y)-coordinates of each root greater than 2 *mm* in diameter which allows for two-dimensional evaluation of root distribution on a large scale. Using this method, small roots with a diameter between 2 and 5 *mm* were assessed in 19 pits on altogether 72 m^2 of soil profiles in monospecific stands of European beech (*Fagus sylvatica* L.) and of Norway spruce (*Picea abies* (L.) Karst.).

Evaluation of the root distribution data by Schmid & Kazda (2001) by the means of a geographical information system showed aggregation of roots between 2 mm and 5 mm diameter in specific soil patches (Schmid & Kazda 2005). They provided some evidence, that these root clusters occur independently from the distance to and the diameter of the neighboring trees. However this evaluation was not able to account for differences in root clustering

between European beech and Norway spruces besides an indication that beech requires less roots to achieve the same degree of clustering as Norway spruce.

The methodological task of the present paper was to test whether point process models can describe the spatial root properties as the root distribution is non-random *per se* due to declining vertical frequency of roots (Parker & van Lear 1996, Schmid & Kazda 2001). Or more specifically, whether after a homogenisation of the root data according to a vertical distribution function, similarly to the one in Schmid & Kazda (2001), the spatial distribution of roots between 2 *mm* and 5 *mm* diameter can be modelled by a homogeneous Poisson process (Stoyan et al. 1995), in other words as a completely spatially random point pattern (notice that a point pattern being a realisation of a Poisson point process is equivalent to a point pattern being completely spatially random, since the location of a point of the point process is independent from the locations of the other points).

Point process characteristics like e.g. the pair correlation function, the L-function and Baddeley's J-function are widely used in the statistical analysis of spatial point patterns (Diggle 2003; Ripley 1981; Stoyan et al. 1995). They offer the possibility to get not only qualitative knowledge about the spatial structure of such point patterns, but to quantify them for specific regions of point-pair distances. Another advantage of these methods compared to alternative techniques of spatial analysis like e.g. Voronoi-tessellations (Marcelpoil & Usson 1992; Okabe et al. 2000) or minimum spanning trees (Dussert et al. 1986, 1987) is their independence of underlying point process intensities i.e. of the average number of points per unit square. Thus point process modelling seems to be suitable especially for root studies where the number of roots found varies within wide ranges and where the underlying vertical distribution is different between the studied species (Schmid & Kazda 2001).

The aim of the presented application of point process modelling to the root data was to quantify the degree of root aggregation in neighbouring mature stands of *Fagus sylvatica* and *Picea abies*. Root clustering in order to exploit a maximum of soil resources was demonstrated for soil water and nutrients P and K by Smucker and Aiken (1992) and Mou et al. (1995), respectively. Investigations of 2D root distribution on trench soil profiles by point process modelling can hereby provide further information for understanding of below-ground processes in mature tree stands. The hypothesis tested is, that under comparable soil properties in these two adjacent stands no differences exist between the clustering of roots in stands of *Fagus sylvatica* and *Picea abies* and thus both species exploit the soil resources with the same intensity.

2. MATERIAL AND METHODS

2.1 Data description

For details of site description, pit excavation and root mapping, see Schmid & Kazda (2001). Investigations in the present paper are based upon this article and thus only a short summary of the most important facts is given.

Data collection took place near Wilhelmsburg, Austria (48°05'51" N, 15°39'48" E) in adjoining pure stands of *Fagus sylvatica* and of planted *Picea abies*. One experimental plot of about 0.5 *ha* was selected within each stand. The sites were similar in aspect (NNE), inclination (10 %) and altitude (480 *m*). The characteristics of the spruce and beech stands, e.g. the age (55 and 65 years), the dominant tree height (27 *m* and 28 *m*) and the stand density (57.3 and 46.6 trees /ha), also were similar to each other. The soils with only thin organic layer (about 4 *cm*) can be classified as stagnic cambisols developed from Flysch sediments. Annual rainfall in Wilhelmsburg averages 843 *mm* with a mean summer precipitation from May to September of 433 *mm*. The mean annual temperature is 8.4° *C*, and the mean summer temperature is 15.7° *C*.

In every stand 10 soil pits with a size of 2×1 *m* were excavated, leading to 20 vertical profile walls of *Fagus sylvatica* and to 16 vertical profile walls of *Picea abies* that are analyzed in the following. Notice that in the case of *Picea abies* only 16 of the 20 profile walls can be used due to failures in data collection.

In most cases 13-19 trees were within a radius of 10 *m* around the pit centre. The minimum distance from the pit centre to the nearest tree ranged from 0.5 *m* to 2.8 *m*. On each wall all coarse roots were identified and divided into living and dead. All living small roots (2-5 *mm*) were marked with pins and digitally photographed. These pictures were evaluated and a coordinate plane was drawn over each profile wall W, so that every root corresponds to a point x_n in the plane. Thus, for each profile wall W, a point pattern $\{x_n\} \subset W$ of root locations was determined.

After the root mapping the images of the profile walls W with area $|W| = 200\ cm \times 100\ cm$ are regarded as realisations of stochastic point processes $\{X_n\}$ in $\mathbf{R}^2$ observed within the sampling window W (Fig. 1).

2.2 Data analysis

Data analysis and simulation was done using the GeoStoch library system. GeoStoch is a Java-based open-library system developed by the Department of Applied Information Processing and the Department of Stochastics of the

University of Ulm which can be used for stochastic-geometric data analysis and spatial statistics (Mayer 2003; Mayer et al. 2004); see also the internet description of this project under http://www.geostoch.de. Statistical comparison of the two groups of data sets was based on the Wilcoxon-Mann-Whitney test, e.g. to compare mean numbers of points (see Section 3.1).

2.3 Vertical homogenisation

The hypotheses, similarly to the ones made in Schmid & Kazda (2001) that the depth densities of the roots of *Picea abies* and *Fagus sylvatica* can be approximated by exponential and gamma distributions, respectively, were tested and the results were satisfactorial. Therefore, in order to be able to assume stationarity and isotropy for models of generating point processes, the data had to be homogenised with respect to the vertical axis. Such a homogenisation is based on the fact that each random variable Y with a continuous distribution function F_Y can be transformed to a uniformly distributed random variable U on the interval $[0,1]$ by

$$U = F_Y(Y). \tag{2.1}$$

Hence, the raw data is processed as follows: Denoting the original depths, the total depth of the sampling window and the obtained transformed depths as h_{orig}, h_{tot} and h_{tran} respectively, the transformed depths h_{tran} are obtained as

$$h_{\text{tran}} = \frac{F^*(h_{\text{orig}})}{F^*(h_{\text{tot}})} h_{\text{tot}}, \tag{2.2}$$

where $F^*(x)$ symbolises the suitable distribution function, i.e. the exponential distribution function in the case of *Picea abies* and the gamma distribution function in the case of *Fagus sylvatica*. The total depth was given as $h_{tot} = 100\ cm$. Therefore, for *Picea abies* we can provide the analytic formula

$$h_{tran}^{spruce} = \frac{1 - e^{-\lambda_{\text{exp}} h_{orig}^{spruce}}}{1 - e^{-100\lambda_{\text{exp}}}} h_{tot}, \tag{2.3}$$

where $\lambda_{\text{exp}}^{-1}$ represents the mean value of the exponential distribution. In the case of *Fagus sylvatica* no analytical formula for h_{tran}^{beech} can be given. Here computations have to be performed numerically. Parameters (λ_{exp} and (α, β), respectively) for the distribution functions $F^*(x)$ are estimated using maximum-likelihood-estimators for each sampling window individually. Notice that in the following, first only preprocessed data is regarded, which

is vertically homogenised (Fig. 1), that means that the vertical coordinate is assumed to be uniformly distributed on $[0, h_{\text{tot}}]$. Later on, the results obtained for homogenised data are re-interpreted for original root data, where an inverse model transformation is used.

2.4 Statistical methods

In order to analyse the given samples of small root point patterns we used estimated point process characteristics. In particular we focused on two functions, namely the pair correlation function and the *L*-function. Additionally the *J*-function was considered for a justification of the results obtained for the two other functionals. Formal definitions of the mentioned functions as well as descriptions of estimators used are provided in Appendix A. Thus only a short explanation of the above mentioned functions is given in this section. Notice that for point pair distances of more than 40 cm estimations become unstable because of the sampling window size and are therefore omitted in the following.

Pair correlation function

In order to define the pair correlation function, the product density of second order $\rho^{(2)}$ has to be introduced first. If two discs C_1 and C_2 are regarded that have infinitesimal areas dF_1, dF_2 and midpoints x_1, x_2 respectively, the probability for having in each disc at least one point of X is approximately equal to $\rho^{(2)}(x_1, x_2)dF_1dF_2$ (Stoyan & Stoyan 1994). Note that in the motion-invariant case the product density of second order $\rho^{(2)}(x_1, x_2)$ can be replaced by $\rho^{(2)}(r)$, where $r = \|x_1 - x_2\|$ is the Euclidean distance between x_1 and x_2. The pair correlation function $g(r)$ is then defined by

$$g(r) = \frac{\rho^{(2)}(r)}{\lambda^2} \tag{1.1}$$

In the case of complete spatial randomness we have that $g_{\text{Poi}}(r) \equiv 1$. A possible interpretation of the pair correlation function is that it reflects the scaled density function for the distances of point pairs. Hence $g(r) > 1$ indicates that there are more point pairs having distance r than in the Poisson case, while $g(r) < 1$ indicates that there are less point pairs of such a distance. To estimate $g(r)$ kernel estimation is used and the bandwidth h of

the Epanechnikov kernel was chosen as $h = c\hat{\lambda}^{-1/2}$ (cf. Appendix A). Several $c \in [0.1, 0.2]$ were used, according to the suggestion given in Stoyan & Stoyan (1994). Since all of them provided similar results, in the following graphs are displayed for $c = 0.15$.

L-function

Since for Poisson processes $K_{\text{Poi}}(r) = \pi r^2$, the K-function is scaled to get a variance-stabilized characteristic, called *L*-function which is equal to r under complete spatial randomness. Therefore $L(r)$ is defined as

$$L(r) = \sqrt{\frac{K(r)}{\pi}} \tag{2.4}$$

and can be estimated by

$$\hat{L}(r) = \sqrt{\frac{\hat{K}(r)}{\pi}}. \tag{2.5}$$

Especially the estimated difference $\hat{L}(r) - r$ is useful for analytical purposes since $L(r) - r$ is identical to 0 in the Poisson case and if it has a positive slope this is a sign of attraction between point pairs of such a distance, while on the other hand if it has a negative slope this is a sign of rejection between point pairs of such a distance.

J-function

In order to validate the results obtained for the pair correlation function and for the *L*-function, Baddeley's *J*-function has been used. Based on the spherical contact distribution function $H_S(r)$ and on the nearest neighbour distribution function $D(r)$, it is defined by

$$J(r) = \frac{1 - H_S(r)}{1 - D(r)}. \tag{2.6}$$

In the case of Poisson point processes we have that $J_{\text{Poi}}(r) \equiv 1$, since then $H_S(r) = D(r)$ because of the independent scattering of points. If $J(r) > 1$, it holds that $D(r) > H_S(r)$ and therefore one can conclude that there is repulsion between point pairs of distance r. On the other hand if $J(r) < 1$, it is true that $D(r) < H_S(r)$ and hence there is attraction between point pairs of distance r compared to the case of complete spatial randomness.

Matérn-cluster point process

The Matérn-cluster point process X_{mc} is based on a Poisson process with intensity λ_p whose points are called parent points. Around each parent point a disc with radius R is taken in which the points of the Matérn-cluster process are scattered uniformly and independently from each other. The number of points in such a disc is Poisson distributed with parameter $\pi R^2 \lambda_d$. Note that λ_d is the mean number of points per unit area generated by a single parent point in a disc of radius R. Since the parent points themselves are not part of the Matérn-cluster process, the intensity of the Matérn-cluster process is given by $\lambda_{\text{mc}} = \pi R^2 \lambda_d \lambda_p$. Thus, the Matérn-cluster point process X_{mc} is uniquely determined by three of the four parameters λ_p, λ_d, R and λ_{mc}. Obviously, for small distances, there is a bigger mean number of points of X_{mc} in a disc around an arbitrarily chosen point of X_{mc} than for Poisson processes of comparable intensity. For X_{mc}, the point process characteristics described in above are known (Stoyan & Stoyan 1994).

Model fitting

After the analysis of estimated point process characteristics, a Matérn-cluster model was fitted to the transformed data. After an estimation of λ_{mc} by using the estimator given in (A.4), the parameters λ_p and R can be estimated by numerical minimisation of the integral

(2.7) $$\int_0^{r_{\max}} (\hat{g}(r) - g_{\text{theo}}(r))^2 dr ,$$

where $\hat{g}(r)$ is the averaged estimated pair correlation function for the Epanechnikov kernel with $c = 0.15$ and $g_{\text{theo}}(r)$ is the theoretical value for the pair correlation function of the Matérn-cluster process with parameters λ_p, R and λ_{mc}. The range has been chosen from $0\ cm$ to $r_{\max} = 50\ cm$, where $r_{\max}$ equals half the minimum of the given depth and width of the sampling window.

3. RESULTS

Notice that in the following the transformed point patterns of spruce and beech were analyzed, which are considered stationary and isotropic.

3.1 Estimated point pattern characteristics

The average number of roots (i.e. points in the sampling window) for profile walls of *Picea abies* is significantly higher than for the profile walls of *Fagus sylvatica* ($\alpha = 0.05$). Since the sampling windows have the same size, a similar result is obtained regarding intensities per cm^2 ($\lambda^{\text{spruce}} = 0.00403$ vs. $\lambda^{\text{beech}} = 0.00262$).

Isotropy was tested by determining the empirical directional distribution of the angles of point pairs to the axes and testing them for uniform distribution. The hypothesis of isotropy could not be rejected ($\alpha = 0.05$), hence in the following isotropy is assumed. The quadrat count method (Stoyan & Stoyan 1994) was used to test on complete spatial randomness. Here, using a 4×4 grid, the hypothesis that the given point patterns are extracts of realisations of homogeneous Poisson processes was rejected ($\alpha = 0.05$). This implies that after the vertical root distributions were compensated by the estimated distribution functions (2.2) roots between 2 and 5 mm diameter are aggregated in specific parts of soil.

It is important to notice that even regarding the number of roots in the profile walls, the variability of root numbers in both groups, spruce and beech, is bigger than between the two groups. Therefore, means for spruce and beech respectively are regarded in the applied functions instead of individual values for each wall investigated. Hence in the following we look at the mean behaviour of the two species. Notice also that it was not tested whether the differences in the plots were statistically significant. For functions the mean was taken in a pointwise sense resulting in mean value functions, where each sample had the same weight. Means based on weighted average estimation (Diggle et al. 2000) were also regarded, but resulted in almost identical graphs, compared to graphs for means using equal weights. They are therefore omitted here.

The graphs for averaged estimated pair correlation functions (Fig. 2) provide strong indication for root clustering, where this effect seems to be stronger for spruce than for beech. For both tree species the estimated pair correlation function runs above *1* for a radius $r < 14\ cm$ and the function for spruce (crosses) is bigger than the function for beech (diamonds) for $r < 9\ cm$.

Graphs for the averaged estimated values of $\hat{L}(r) - r$ are shown in Fig. 3. Since in the Poisson case $L(r) = r$ a positive slope means that there is an attraction, while a negative slope indicates repulsion. Again there are signs of attraction for small distances, less than $9.5\ cm$ and less than $13.5\ cm$ respectively, and the attraction seems to

be stronger for spruce (crosses) compared to beech (diamonds) since the slope of $\hat{L}(r)-r$ is bigger. Fig. 3 indicates further that less point pairs for beech occur in a range between about $12\ cm$ and $40\ cm$.

Averaged estimated *J*-functions for both groups (Fig. 4) give clear indication for attraction between point pairs of a distance less than $12\ cm$, since both functions are below 1 in this region and have a negative slope. A second observation is that the line for spruce (crosses) lies beneath the line for beech (diamonds), which means that root pairs of spruce are more attracted to each other than roots of beech for such distances. Notice that for radii larger than $20\ cm$ the estimator becomes numerically unstable, and therefore should not be taken into further consideration. Also one should keep in mind that the *J*-function is the quotient of two cumulative quantities, that means that often the slope of the *J*-function is more of interest than the absolute value at a specific point pair distance *r*.

All regarded estimated point pattern characteristics show that there are strong signs of clustering effects for roots at a distance of less than about $12\ cm$ and that the clustering seems to be stronger for spruce compared to beech, but in a smaller cluster region. Additionally by looking at the estimated *L*-function, it can be seen that for beech and distances of less than $0.5\ cm$ there seems to be a slight repulsion effect, since $\hat{L}(r)-r<0$ for $r\le 0.5cm$. Another interesting observation is that in a range between $12\ cm$ and $40\ cm$ the number of point pairs in beech stands is reduced compared to the number of point pairs in spruce stands.

3.2 Fitting of the Matérn-cluster model

Regarding the results of the estimated point process characteristics described in Section 3.1 and because of its simplicity, Matérn-cluster processes are chosen as a model for the underlying point processes. This model is fitted to the transformed data and the parameter λ_{mc}, indicating the root intensity, is estimated as in (A.4), resulting in $\widehat{\lambda_{\mathrm{mc}}}^{\mathrm{spruce}}=0.00403$ and $\widehat{\lambda_{\mathrm{mc}}}^{\mathrm{beech}}=0.00262$. After the estimation of λ_{mc} for the roots of both species, minimisations of the integral given in (2.7) yield estimates for R and λ_p. The obtained parameters are $\hat{R}^{\mathrm{spruce}}=4.9\ cm$ and $\widehat{\lambda_p}^{\mathrm{spruce}}=0.00690$ for spruce roots, while for beech roots they are $\hat{R}^{\mathrm{beech}}=7.4\ cm$ and

$\widehat{\lambda}_p^{\text{beech}} = 0.00603$. The parameter R indicates different ranges of attraction for roots between $2\text{-}5\,mm$ diameter at smaller cluster regions for spruce than for beech.

The given point patterns are modelled as extracts of realisations of stationary Matérn-cluster processes with intensities $\lambda_{\text{mc}}^{\text{spruce}} = 0.00403$ and $\lambda_{\text{mc}}^{\text{beech}} = 0.00262$, with cluster radii $R^{\text{spruce}} = 4.9\,cm$ and $R^{\text{beech}} = 7.4\,cm$, and with parent-process intensities $\lambda_p^{\text{spruce}} = 0.00690$ and $\lambda_p^{\text{beech}} = 0.00603$. In order to get an idea for the degree of clustering, the quantity

$$\lambda_d = \frac{\lambda_{\text{mc}}}{\lambda_p \pi R^2} \tag{3.1}$$

was evaluated. For *Picea abies* one gets $\lambda_d^{\text{spruce}} = 0.00774$, while for *Fagus sylvatica* $\lambda_d^{\text{beech}} = 0.00253$ is obtained. These parameters allow us to conclude that there is stronger clustering within a smaller cluster radius for spruce roots, while for the beech roots the clustering is substantially weaker.

These models were validated by Monte-Carlo tests. The estimated Matérn-cluster models were simulated 200 times and the pair correlation functions were estimated to get 95 % envelopes for the pair correlation functions of the data. Since the pair correlation functions of spruce (Fig. 5a) and beech (Fig. 5b) lies between these envelopes, the Matérn-cluster models fit well to the data. For *L*-functions similar results were obtained and are omitted here.

In Figs 6a and 7a realisations of the homogeneous Matérn-cluster models are displayed, utilising the estimated model parameters of *Picea abies* and *Fagus sylvatica*, respectively. In Figs 6b and 7b the discs, in which the points are scattered uniformly and independently, are displayed. After the inverse transformations (cf. Appendix B), the corresponding inhomogeneous Matérn-cluster models are obtained. The results of the inverse transformation are visualised in Figs 6c, 6d, 7c and 7d. Structures originating from the inversely transformed data shown in the upper part of Figs 6d and 7d suggest clusters with the longest extension along the horizontal axis. The lower part of Figs 6d and 7d should not be used for structural interpretation however since the data transformation and retransformation of the sparsely distributed roots dominates the original spatial structure in larger soil depths.

4. DISCUSSION

The point process characteristics using the transformed data described the two dimensional distributions of small roots (2 - 5 mm diameter) in pure stands of *Picea abies* and *Fagus sylvatica*. As a first characteristic, estimated pair correlation functions have been analysed. Afterwards in order to get a validation for the results as well as to get further information, the function $\hat{L}(r)-r$ has been applied. Finally, estimated *J*-functions were taken into account to get another proof for the inferences made. This approach of looking at several different characteristics has obvious advantages, since conclusions derived from several independently calculated parameters are more profound and can elucidate such specific behaviour like the repulsion effect for very small beech root distances.

In forest soils, there is a pronounced gradient of nutrient turn-over providing the highest availability in the topsoil. This is true for the investigated stands, where the fine roots of both species showed the highest biomass of 600 - 800 g m^{-3} in 0 and 10 cm soil depth (Schmid 2002). The small roots of spruce followed the same distribution whereas beech small roots showed the highest abundance between 10 and 20 cm soil depth (Schmid & Kazda 2001). After small root positions within the trench soil profiles (i.e. points within a sampling window) were homogenised (transformed) using the specifically calculated distribution function (2.2), the averaged estimated pair correlation functions (Fig. 2) show that attraction can be observed for point pairs with distances less than approximately 14 cm. This means that roots of both species tend to cluster in areas up to this diameter. As roots react to nutrient enriched soil patches by enhanced growth and greater biomass in these areas (Drew 1975; Morris 1996), this attraction of roots within this diameter could also be a direct link to a local occurrence of soil resources. These inferences were validated further by estimated *J*-functions revealing root clustering at pair distances below 12 cm (see Fig. 4). Here we want to stress once more the fact that the estimated functions are pointwise means of the estimations for the individual sample windows.

The estimated function $\hat{L}(r)-r$ (Fig. 3) indicates that the number of roots (point pairs) with a distance between 12 cm and 40 cm was reduced in the case of *Fagus sylvatica*, while for *Picea abies* the number of roots of such a distance was more like in the case of a Poisson process, indicated by function values oscillating between 2 and 2.5 for distances more than 10 cm (Fig. 3). Whereas no interaction between the clusters themselves was found for Norway spruce, slight rejection between the root clusters occurred for European beech. Such avoidance of competition for resources was reported also for roots of Sweetgum and Loblolly pine, which showed a tendency to avoid overlap with roots of other plant while foraging for nutrients (Mou et al. 1995). In this context it is important

to notice that these structural differences are independent of the observed significant difference in the average number of roots for *Picea abies* and *Fagus sylvatica*.

The homogenised point patterns were modelled as Matérn-cluster processes that have some serious advantages. Besides certain simplicity and known theoretical values for point process characteristic, the sample data were fitted well by this model (Fig. 5). The estimated point process characteristics using the Matérn-cluster processes further differentiated between the species. The results show for spruces a stronger clustering in a smaller range of attraction ($R^{\text{spruce}} = 4.9\ cm$), while the clustering is weaker for beeches, but the range of attraction ($R^{\text{beech}} = 7.4\ cm$) seems to be larger. This finding is in accordance with another investigation calculating influence areas for each root by Schmid & Kazda (2005). Their results indicated that the root system of spruce requires more roots to achieve a similar degree of space acquisition and thus beech exploits patchily distributed soil resources at lower root numbers. Furthermore, the evaluation of the diameter growth of coarse roots (> 5 mm) found that growth rates of beech roots exceeded those of spruce by up to 25 % (Schmid & Kazda 2001). Results of both investigations provide an evidence for higher growth and more efficient space acquisition by roots of European beech compared to Norway spruce. From the structural point of view, there is a combination of two effects, the depth distribution, similarly described in Schmid & Kazda (2001) and the cluster effects quantified in the present paper.

Stronger clustering in the case of spruce than in the case of beech can be also seen regarding the characteristics mentioned above as well as by a comparison of the estimated parameters for the homogeneous model $\lambda_d^{\text{spruce}} = 0.00774$ vs. $\lambda_d^{\text{beech}} = 0.00253$, which are measures for the degree of clustering in a specific cluster. These substantial differences between the species is significant as the average numbers of cluster regions are almost equal ($\widehat{\lambda}_p^{\text{spruce}} = 0.00690$ vs. $\widehat{\lambda}_p^{\text{beech}} = 0.00603$). The previous GIS-based investigation of root distribution (Schmid & Kazda 2005) was not able to quantify the differences of clustering between the two species as precisely as the applied modelling by point processes. Stronger root clustering of spruce can be seen as an indication of more intensive intraspecific competition than in the case of beech. This is supported by a structural link established by Schmid (2002) between fine and coarse roots in the two investigated stands providing an identical ratio between the biomass of fine and coarse roots of 0.9. The same ratio between fine and coarse roots suggests therefore higher abundance of fine roots in spruce clusters and thus more intensive intraspecific competition (Smucker & Aiken 1992) in spruce than in beech. Beech also requires fewer roots than spruce to achieve the same degree of root clustering (Schmid & Kazda 2005) and the clustering is weaker but the range of attraction larger as indicated by the

parameters of the fitted Matérn-cluster processes. Furthermore beech root clusters themselves seem to avoid an overlap which together with the clustering characteristics described above indicates a more sophisticated rooting system than in the case of Norway spruce.

The non-homogeneous Matérn-cluster model constructed by a retransformation of the homogeneous model reflected the observed depth distribution of the tree roots. The visualisation of the retransformed data suggests a depth-dependent size and shape of root clusters. Close to the soil surface, roots form clusters along the horizontal axis. This shape agrees also with the horizontally distributed root points in the original samples (Figs 1a and 1c). Horizontally growing roots as well as the shape of generated clusters may reflect the attractive soil patches in the nutrient-rich topsoil layers. Deeper, the real size of clusters is larger and more circular. However, because the transformation and retransformation of root data at low intensities in the deep parts of the soil profile makes the results unstable, the lower third of Figs 6d and 7d are not really useful for interpretation of spatial structures. The small roots investigated in this study were described regarding water and nutrient uptake (Lindenmair et al. 2001) and they mediate to the most active fine roots (< 2 *mm*). Thus, clusters of small roots reflect the presence of nutrient patches or zones of better water availability (Jackson & Caldwell 1993; Parker & Lear 1996; Ryel et al. 1996). As the number of small roots and their clustering was independent of the distance to the surrounding trees and of their diameter (Schmid & Kazda 2005), the root clusters are suggested as an inherent property of below-ground space acquisition.

The method of data collection provided an exceptionally large amount of data describing the spatial distributions of roots and thereby enabled us to perform a statistical analysis of the random spatial distributions by the usage of point pattern characteristics. Summarizing the structures found, we can state that after root abundances were compensated vertically, spatial distribution of roots for both tree species is still not completely random. Returning to the hypothesis postulated in the introduction, we have quantified the degree of clustering as well as the size of the cluster region by a model fitting and parameter estimation for Matérn-cluster models with respect to transformed data. Looking at the real data, of course we have a mixing of the effects detected for the transformed case and the given depth distributions that were assumed as being exponentially distributed in the case of *Picea abies* and as being gamma-distributed in the case of *Fagus sylvatica* (Schmid & Kazda 2001). A reason for such clustering effects is seen in the inhomogeneity of soil resources. Therefore a simultaneous spatial analysis of root and nutrient distribution would be very interesting, in order to test the concomitant root and nutrient heterogeneity in different regions of natural soils.

Acknowledgement

The data collection was financially supported by the Austrian Science Foundation within the Special Research Program "Restoration of Forest Ecosystems", F008-08. Stefanie Eckel is supported by a grant of the graduate college 1100 at the University of Ulm. We would like to thank the two referees for their very precise and detailed comments that were of great help for us.

REFERENCES

Böhm, W. 1976. In site estimation of root length at natural soil profiles. J. Agric. Sci. **87**: 365-368.

Bouillet, J.-P., Laclau, J.-P., Arnaud, M., Thongo M'Bou, A., Saint-André, L. & Jourdan, C. 2002. Changes with age in a spatial distribution of roots of Eucalyptus clone in Congo - Impact on water and nutrient uptake. Forest Ecol. and Manage **171**: 43-57.

Caldwell, M.M., Manwaring, J.H. & Durham, S.L. 1996. Species interaction at the level of fine roots in the field: influence of soil nutrient heterogeneity and plant size. Oecologia **106**: 440-447.

Diggle, P.J. 2003. Statistical Analysis of Spatial Point Patterns. Oxford University Press, Oxford.

Diggle, P.J., Mateu, J. & Clough, H.E. 2000. A comparison between parametric and non-parametric approaches to the analysis of replicated spatial point patterns. Adv. Appl. Prob. **32**: 331-343.

Drew, M.C. 1975. Comparison of the effects of a localised supply of phosphate, nitrate, ammonium and potassium on the growth of the seminal root system, and the shoot, of barley. New Phytol **75**: 479-490.

Dussert, C., Rasigni, G., Rasigni, M., Palmari, J. & Llebaria, A. 1986. Minimal spanning tree: a new approach for studying order and disorder. Physical Revue B **34**: 3528-3531.

Dussert C., Rasigni, G., Palmari, J., Rasigni, M. Llebaria, A. & Marty, F. 1987. Minimal spanning tree analysis of biological structures. Journal of Theoretical Biology **125**: 317-323.

Facelli, E. & Facelli, J.M. 2002. Soil phosphorus heterogeneity and mycorrhizal symbiosis regulate plant intra-specific competition and size distribution. Oecologia **133**: 54-61.

Hölscher, D., Hertel, D., Leuschner, C. & Hottkowitz, M. 2002. Tree species diversity and soil patchiness in a temperate broad leaved forest with limited rooting space. Flora **197**: 118-125.

Jackson, R. B. & Caldwell, M. M. 1993. Geostatistical patterns of soil heterogeneity around individual perennial plants. J. Ecol. **81**: 683-692.

Jackson, R. B. & Caldwell, M. M. 1996. Integrating resource heterogeneity and plant plasticity: modelling nitrate and phosphate uptake in a patchy soil environment. J. Ecol. **84**: 891-903.

Krauss, G., Müller, K., Gärtner, G., Härtel, F., Schanz, H. & Blanckmeister, H. 1939. Standortsgemäße Durchführung der Abkehr von der Fichtenwirtschaft im nordwestsächsischen Niederland. Tharandter Forstl. Jahrbuch **90**: 481-715.

Lindenmair, J., Matzner, E., Göttlein, A., Kuhn, A.J. & Schröder, W.H. 2001. Ion exchange and water uptake of coarse roots of mature Norway spruce trees (Picea abies L. Karst.). *In*: Plant Nutrition - Food Security and Sustainability of Agro-Ecosystems *edited by* Horst W. J. et al, Kluwer Academic Publishers.

Linkohr, B.I., Williamson, L.C., Fitter, A.H. & Leyser, H.M.O. 2002. Nitrate and phosphate availability and distribution have different effects on root system architecture of Arabidopsis. Plant J. **29**: 751-760.

Marcelpoil, R. & Usson, Y. 1992. Methods for the study of cellular sociology: voronoi diagrams and parametrisation of the spatial relationships. Journal of Theoretical Biology **154**: 359-369.

1 Mayer, J. 2003. On quality improvement of scientific software: Theory, methods, and application in the GeoStoch development.
2 Doctoral Dissertation, University of Ulm.
3 Mayer, J., Schmidt, V. & Schweiggert, F. 2004. A unified simulation framework for spatial stochastic models. Simulation
4 Modelling Practice and Theory **12**: 307-326.
5 Morris, E.C. 1996. Effect of localized placement of nutrients on root-thinning in self-thinning populations. Ann. Bot. **78**: 353-
6 364.
7 Mou, P., Jones, R. H., Mitchell, R. J. & Zutter, B. 1995. Spatial distribution of roots in Sweetgum and Loblolly Pine
8 monocultures and relations with above-ground biomass and soil nutrients. Functional Ecology **9**: 689-699.
9 Okabe, A., Boots, B., Sugihara, K. & Chiu, S.N. 2000. Spatial Tessellations. J. Wiley & Sons, Chichester.
10 Parker, M.M. & Lear, D.H. van 1996. Soil heterogeneity and root distribution of mature loblolly pine stands in piedmont soils.
11 Soil Sci. Society Am. J. **60**: 1920-1925.
12 Pellerin, S. & Pages, L. 1996. Evaluation in field conditions of a three-dimensional architectural model of the maize root system:
13 Comparison of simulated and observed horizontal root maps. Plant & Soil **178**: 101-112.
14 Ripley, B. D. 1981. Spatial Statistics. J. Wiley & Sons, Chichester.
15 Ryel, R.J., Caldwell, M.M. & Manwaring, J.H. 1996. Temporal dynamics of soil spatial heterogeneity in sagebrush-wheatgrass
16 steppe during a growing season. Plant Soil **184**: 299-309.
17 Schmid I. 2002. The influence of soil type and interspecific competition on the fine root system of Norway spruce and European
18 beech. Basic Appl. Ecol. **3**: 339-346.
19 Schmid, I. & Kazda, M. 2001. Vertical distribution and radial growth of coarse roots in pure and mixed stands of *Fagus*
20 *sylvatica* and *Picea abies*. Canadien Journal of Forest Research **31**: 539-548.
21 Schmid, I. & Kazda, M. 2005. Clustered root distribution in mature stands of *Fagus sylvatica* and *Picea abies*. Oecologia, in
22 press.
23 Smucker, A. J. M. & Aiken, R. M. 1992. Dynamic root responses to water deficits. Soil Science **154**: 281-289.
24 Stoyan, D., Kendall, W.S. & Mecke, J. 1995. Stochastic Geometry and its Applications. J. Wiley & Sons, Chichester.
25 Stoyan, D. & Stoyan, H. 1994. Fractals, Random Shapes and Point Fields. Methods of Geometrical Statistics. J. Wiley & Sons,
26 Chichester.
27 Tardieu, F. 1988. Analysis of the spatial variability of maize root density. Plant Soil **107**: 259-266.
28 Wijesinghe, D.K. & Hutchings, M.J. 1997. The effects of spatial scale of environmental heterogeneity on the growth of a clonal
29 plant: an experimental study with Glechoma hederacea. J. Ecol. 85: 17-28.

FIGURE CAPTIONS

Figure 1. Sample of small root distribution for *Picea abies* (original (a), transformed (b)) and for *Fagus sylvatica* (original (c), transformed (d)).

Figure 2. Averaged estimated pair correlation functions for *Picea abies* (crosses) and *Fagus sylvatica* (diamonds). The line $g(r) \equiv 1$ is the pair correlation function in case of the Poisson point process.

Figure 3. Averaged estimated functions $\hat{L}(r) - r$ for *Picea abies* (crosses) and *Fagus sylvatica* (diamonds).

Figure 4. Averaged estimated J-functions for *Picea abies* (crosses) and *Fagus sylvatica* (diamonds).

Figure 5. Estimated mean pair correlation function of *Picea abies* (a) and *Fagus sylvatica* (b). The 95 % envelopes displayed are based on Matérn-cluster processes with fitted parameters.

Figure 6. Realization of the homogeneous Matérn-cluster model, showing the daughter points (a) and the cluster regions (b). A realization (c) of the inhomogeneous Matérn-cluster model for *Picea abies*. Retransformation of the discs around the daughter points (d).

Figure 7. Realization of the homogeneous Matérn-cluster model, showing the daughter points (a) and the cluster regions (b). A realization (c) of the inhomogeneous Matérn-cluster model for *Fagus sylvatica*. Retransformation of the discs around the daughter points (d).

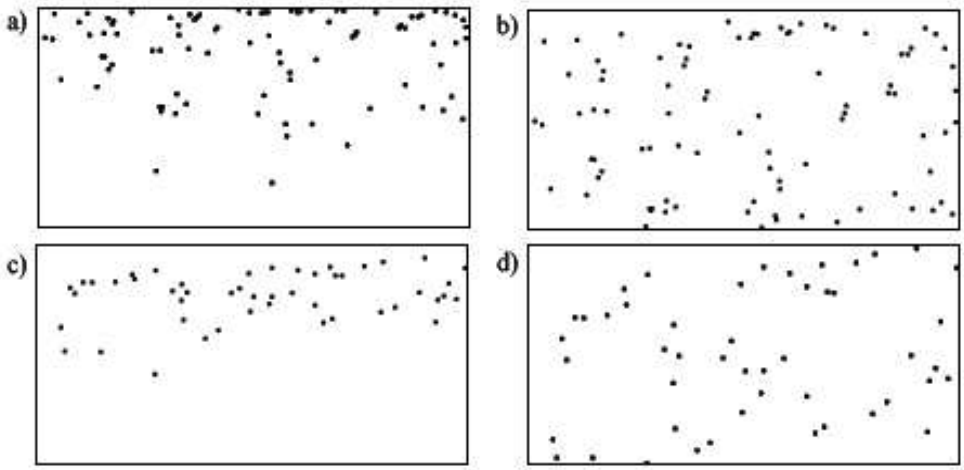

Fig. 1

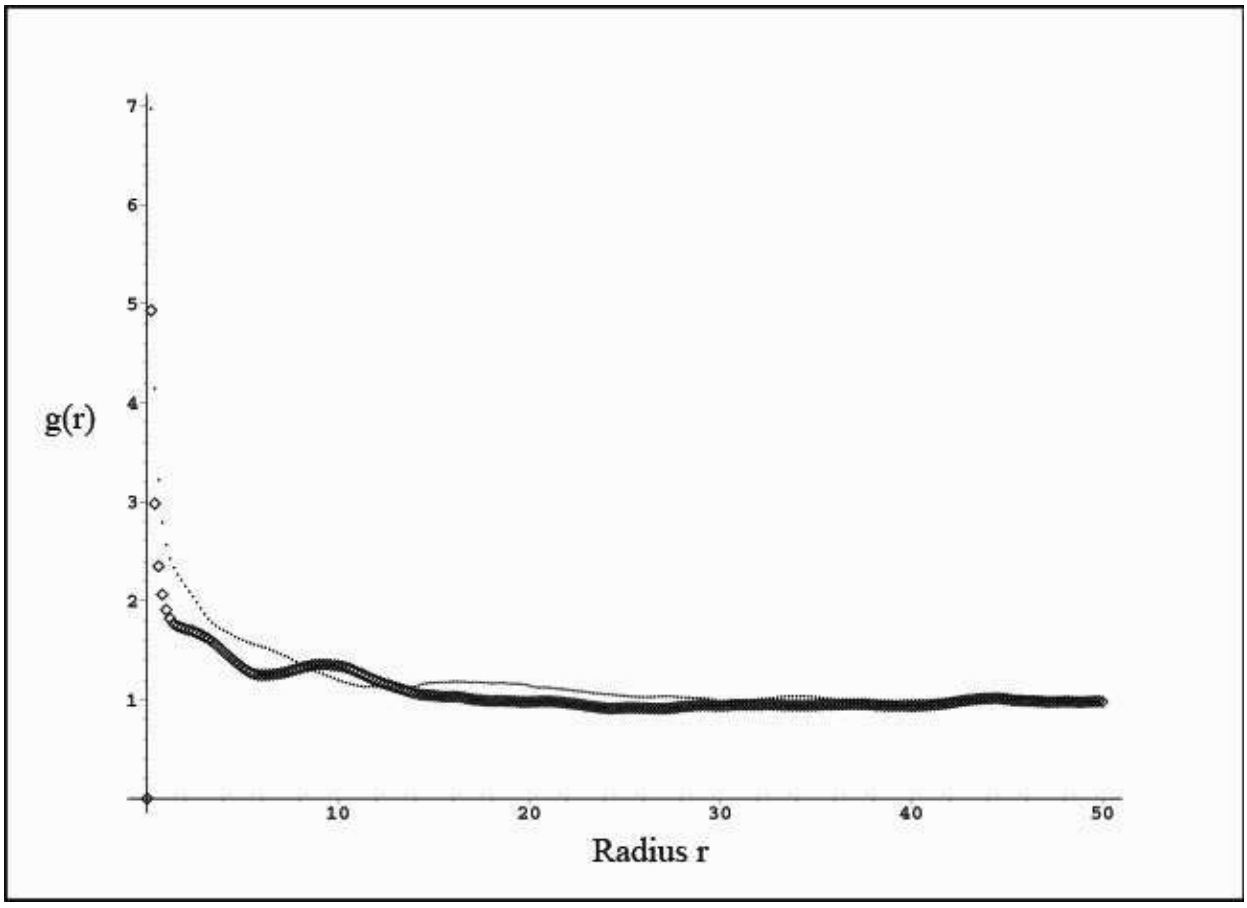

Fig. 2

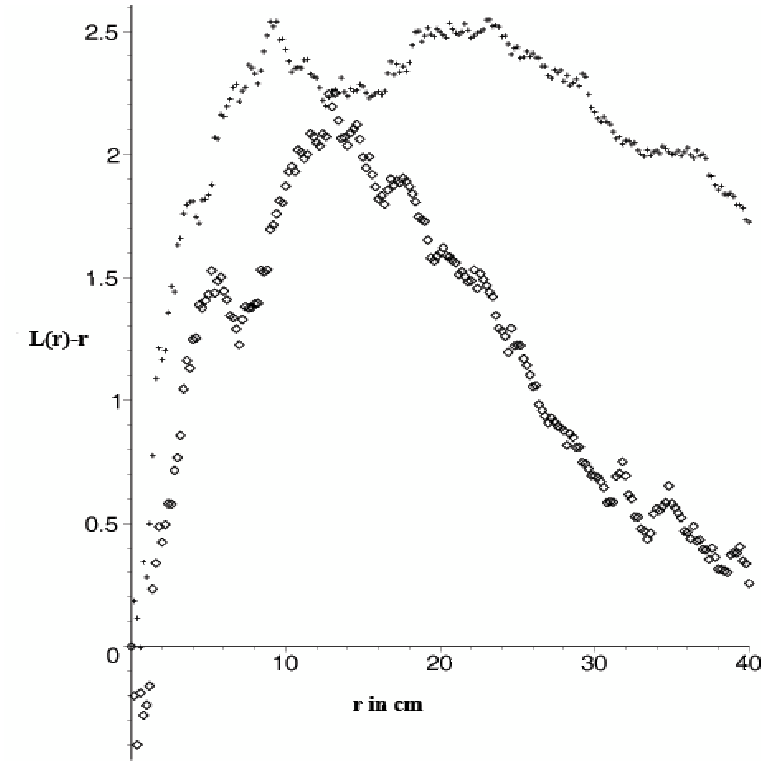

Fig. 3

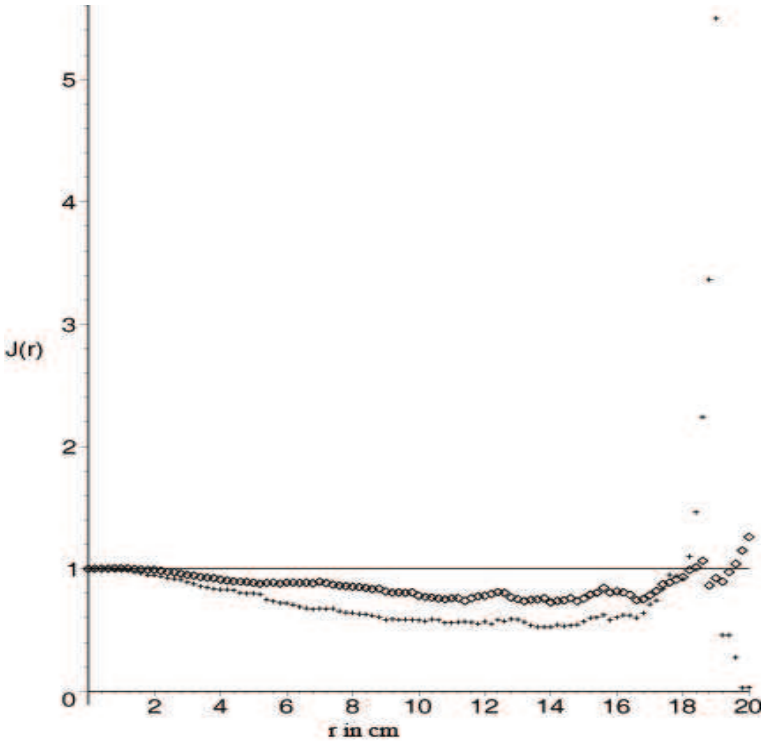

Fig. 4

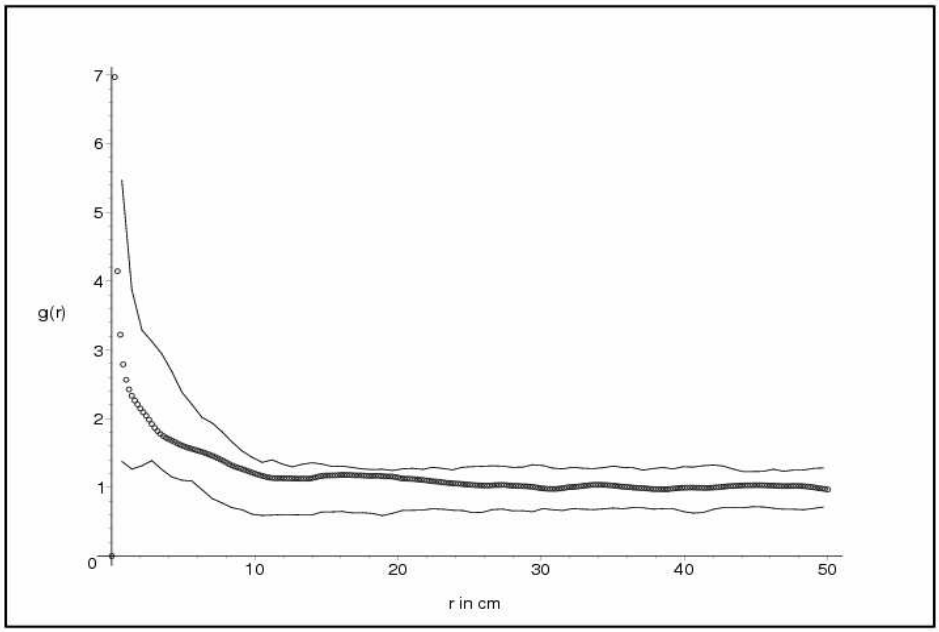

Fig. 5a

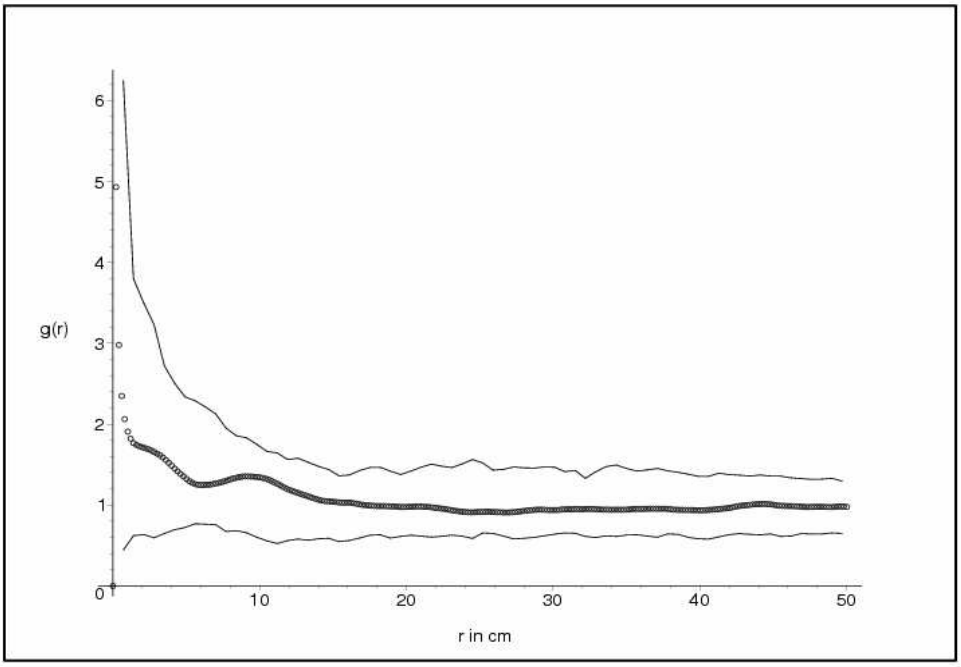

Fig. 5b

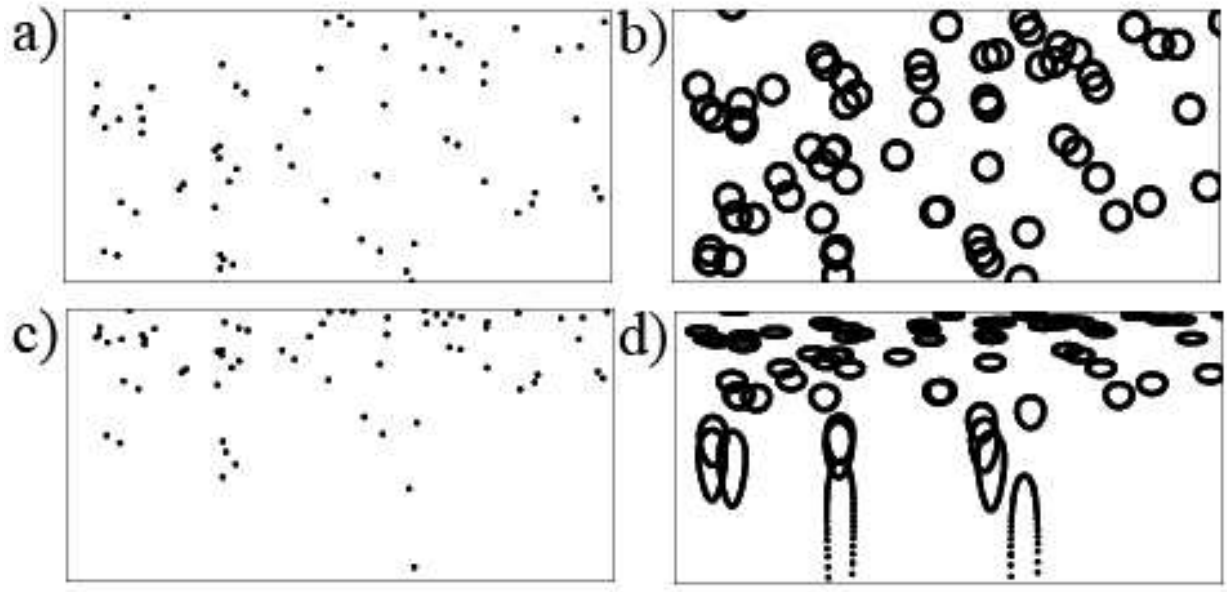

Fig. 6

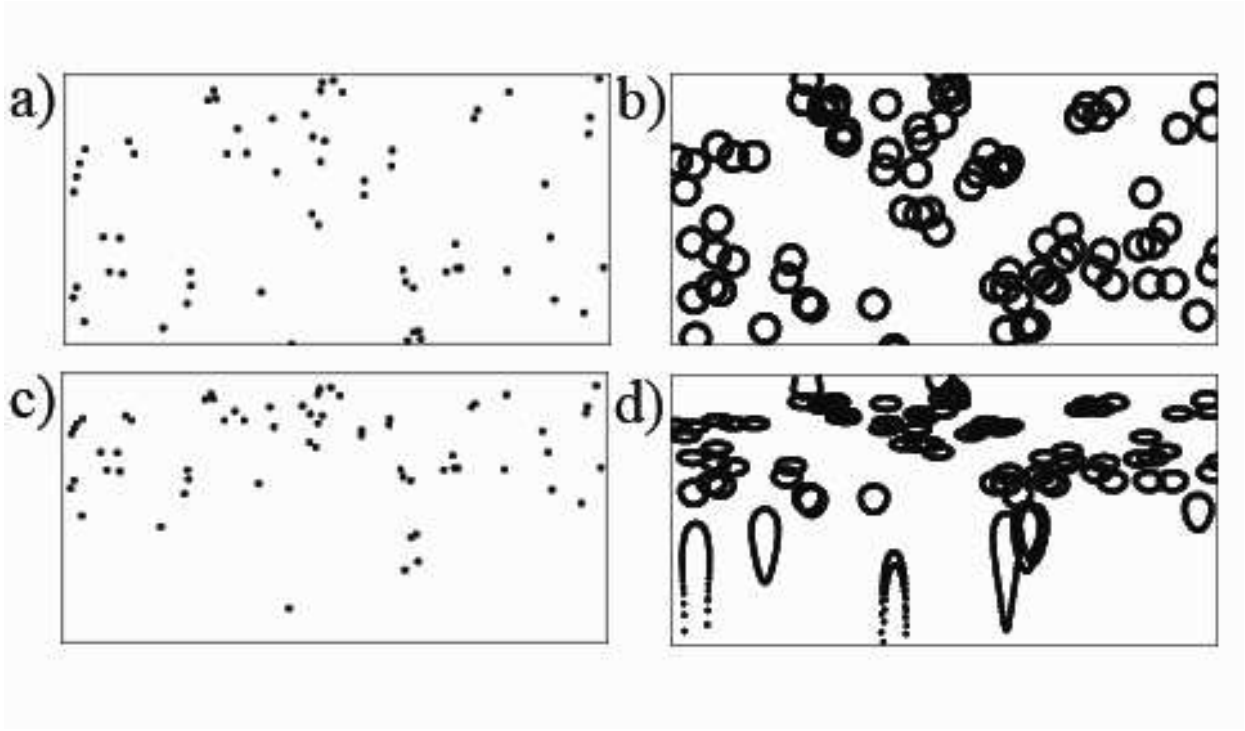

Fig. 7

APPENDIX

A. Point process characteristics and their estimators

In the following let $X = \{X_n\}$ be a point process in $\mathbf{R}^2$ and let $X(W) = \#\{n : X_n \in W\}$ denote the random number of points X_n of X located in a window W. The point process X is called stationary if the distribution of X is invariant under translation and X is called isotropic if the distribution of X is invariant under rotation about the origin.

Intensity

The intensity measure Λ is defined as

(A.1) $$\Lambda(W) = EX(W)$$

for a given set W, where E denotes expectation. Hence $\Lambda(W)$ is the mean number of points in W. Often it is possible to express the intensity measure in terms of an intensity function $\lambda(x)$, where

(A.2) $$\Lambda(W) = \int_W \lambda(x)dx.$$

In the stationary case it suffices to regard an intensity λ since then

(A.3) $$\Lambda(W) = \lambda|W|,$$

where $|W|$ denotes the area of W. A natural estimator for λ is given by

(A.4) $$\hat{\lambda} = \frac{X(W)}{|W|}.$$

According to Stoyan & Stoyan (1994), an appropriate estimator for λ^2 is

(A.5) $$\widehat{\lambda^2} = \frac{X(W)(X(W)-1)}{|W|^2},$$

since even in the case of complete spatial randomness $(\hat{\lambda})^2$ is not an unbiased estimator for λ^2. In the following let the point process X be motion-invariant, i.e. stationary and isotropic.

Pair correlation function

As an estimator for $\rho^{(2)}$,

(A.6) $$\widehat{\rho^{(2)}}(r) = \frac{1}{2\pi r} \sum_{X_i, X_j \in W,\, i \neq j} \frac{k_h(r - \|X_i - X_j\|)}{|W_{X_i} \cap W_{X_j}|}$$

is used (Stoyan & Stoyan 2000), where $\|X_i - X_j\|$ denotes the Euclidean distance between two points X_i and X_j. The term $|W_{X_i} \cap W_{X_j}|$ is an edge correction term, where $W_{X_j} = \{x + X_j : x \in W\}$ is the window W translated by the point X_j, the sum extends over all pairs of points $X_i, X_j \in W$ with $i \neq j$, and $k_h(x)$ denotes the Epanechnikov kernel

(A.7) $$k_h(x) = \frac{3}{4h}\left(1 - \frac{x^2}{h^2}\right) I_{(-h,h)}(x)$$

with bandwidth *h*. The product density $\rho^{(2)}(r)$ is used to obtain the pair correlation function $g(r)$ as

(A.8) $$g(r) = \frac{\rho^{(2)}(r)}{\lambda^2}.$$

The pair correlation function can be estimated by using the estimators for $\rho^{(2)}(r)$ and λ^2.

L-function

The *L*-function is a scaled version of Ripley's *K*-function which is defined such that $\lambda K(r)$ is the mean number of points of the stationary point process X within a ball $b(X_n, r)$ centred at a randomly chosen point X_n of X which itself is not counted (Ripley 1981). As a formal definition one gets

(A.9) $$\lambda K(r) = E \sum_{X_n \in W} \frac{X(b(X_n, r)) - 1}{\lambda |W|}.$$

A possible estimator for $K(r)$ is given by

(A.10) $$\hat{K}(r) = \frac{\kappa(r)}{\widehat{\lambda^2}},$$

where

(A.11) $$\kappa(r) = \sum_{X_i, X_j \in W,\, i \neq j} \frac{I_{b(o,r)}(X_j - X_i)}{|W_{X_j} \cap W_{X_i}|},$$

where $\left|W_{X_i} \cap W_{X_j}\right|$ is an edge correction term. Recall that $\widehat{\lambda^2}$ is the estimator given in (A.5). The *L*-function is then defined by

(A.12) $$L(r) = \sqrt{\frac{K(r)}{\pi}}$$

and can be estimated by

(A.13) $$\hat{L}(r) = \sqrt{\frac{\hat{K}(r)}{\pi}}.$$

J-function

In order to define the *J*-function, the contact distribution function $H_s(r)$ and the nearest neighbour distance distribution function $D(r)$ have to be introduced first. The spherical contact distribution function $H_s(r)$ is defined by

(A.14) $$H_s(r) = 1 - P(X(b(o,r)) = 0)$$

and can be interpreted as the distribution function of the random distance from an arbitrary point outside of X to its nearest neighbour in X. The nearest neighbour distance distribution function $D(r)$ is the distribution function of the distance from a randomly chosen point X_n of X to its nearest neighbour. In the case of complete spatial randomness we have that

(A.15) $$H_s(r) = D(r) = 1 - \exp(-\lambda\pi r^2).$$

The J-function is defined by

(A.16) $$J(r) = \frac{1 - H_s(r)}{1 - D(r)},$$

where

(A.17) $$\hat{J}(r) = \frac{1 - \hat{H}_s(r)}{1 - \hat{D}(r)}$$

is a natural estimator for $J(r)$ with estimators $\hat{H}_S(r)$ and $\hat{D}(r)$ for $H_S(r)$ and $D(r)$, respectively, as considered e.g. in Lieshout & Baddeley (1996).

B. Inhomogeneous Matérn-cluster model

For the original data, which shows a vertical distribution property, the Matérn-cluster model fitted for the homogeneous case has to be retransformed, where the inverse transformation

(B.1) $$h_{\text{orig}} = (F^*)^{-1}\left(\frac{F^*(h_{\text{tot}})}{h_{\text{tot}}} h_{\text{tran}}\right)$$

of the depth is considered, with $(F^*)^{-1}(y)$ representing the generalised inverse function of $F^*(x)$. So for example in the case of *Picea abies* an exponential depth distribution is assumed and therefore

(B.2) $$h_{orig}^{spruce} = -\frac{1}{\lambda_{\text{exp}}} \ln\left(1 - h_{tran}^{spruce} \frac{1 - e^{-100\lambda_{\text{exp}}}}{100}\right),$$

where $\lambda_{\text{exp}}^{-1}$ is the mean value of the exponential distribution. Thereby it is possible to define a retransformed model, where the parent process is given by an inhomogeneous Poisson process with intensity function

(B.3) $$\lambda_p(x, y) = \lambda_p(y) = \lambda_p \frac{f^*(y)}{F^*(h_{\text{tot}})} h_{\text{tot}},$$

where x and y represent the horizontal and vertical coordinate, $f^*(x)$ is the density function of the suitable distribution function $F^*(x)$ (exponential distribution for spruce and gamma distribution for beech), λ_p is the intensity of the parent process of the homogeneous model and h_{tot} represents the total depth of the sampling window. In this model the cluster regions are no longer circles, but the images of these circles under the mapping given in (B.1). They can be written as

(B.4) $$\{(x, y) : (x - x_p)^2 + (F^*(y) - F^*(y_p))^2 \left(\frac{h_{\text{tot}}}{F^*(h_{\text{tot}})}\right)^2 \le R^2\},$$

where the corresponding parent point is denoted by (x_p, y_p). Since the mean total number of points in the given window as well as the mean total number of points in a cluster stay the same compared to the homogeneous model, the intensity function for the inhomogeneous Matérn-cluster point process is given as

(B.5) $$\lambda_{\text{mc}}(x, y) = \lambda_{\text{mc}}(y) = \lambda_{mc} \frac{f^*(y)}{F^*(h_{\text{tot}})} h_{\text{tot}},$$

where λ_{mc} is the corresponding intensity of the homogeneous model.

APPENDIX REFERENCES

Lieshout, M.C. van & Baddeley, A.J. 1996. A nonparametric measure of spatial interaction in point patterns. Statistic Neerlandica **50**: 344-361.

Ripley, B. D. 1981. Spatial Statistics. J. Wiley & Sons, Chichester.

Stoyan, D. & Stoyan, H. 1994. Fractals, Random Shapes and Point Fields. Methods of Geometrical Statistics. J. Wiley & Sons, Chichester.